Electroanatomical Characteristics of Idiopathic Left Ventricular Tachycardia and Optimal Ablation Target during Sinus Rhythm: Significance of Preferential Conduction through Purkinje Fibers

Junbeom Park,[1] Young-Hoon Kim,[2] Chun Hwang,[3] and Hui-Nam Pak[1]

[1]Department of Cardiology, Yonsei University Health System, Seoul;
[2]Korea University Cardiovascular Center, Seoul, Korea.
[3]Utah Valley Regional Medical Center, Provo, UT and Krannert Heart Institute, Indiana University, Indianapolis, IN, USA.

Purpose: We hypothesized that Purkinje potential and their preferential conduction to the left ventricle (LV) posteroseptum during sinus rhythm (SR) are part of reentrant circuits of idiopathic left ventricular tachycardia (ILVT) and reentry anchors to papillary muscle. **Materials and Methods:** In 14 patients with ILVT (11 men, mean age 31.5±11.1 years), we compared Purkinje potential and preferential conduction during SR with VT by non-contact mapping (NCM). If clear Purkinje potential$_{(SR)}$ was observed in the LV posteroseptum and the earliest activation site (EA) of preferential conduction at SR (EA$_{SR}$) was well matched with that of VT (EA$_{VT}$), EA$_{SR}$ was targeted for radiofrequency catheter ablation (RFCA). Also, the anatomical locations of successful ablation sites were evaluated by echocardiography in five additional patients. **Results:** 1) All induced VTs exhibited clear Purkinje potential$_{(VT)}$ and preferential conduction in the LV posteroseptum. The Purkinje potential$_{(VT)}$ and EA$_{VT}$ was within 5.8±8.2 mm of EA$_{SR}$. However, the breakout sites of VT were separated by 30.2±12.6 mm from EA$_{VT}$ to the apical side. 2) Purkinje potential$_{(SR)}$ demonstrated a reversed polarity to Purkinje potential$_{(VT)}$, and the interval of Purkinje potential$_{(SR)}$-QRS was longer than the interval of Purkinje potential$_{(VT)}$-QRS ($p<0.02$) 3) RFCA targeting EA$_{SR}$ eliminated VT in all patients without recurrence within 23.3±7.5 months, and the successful ablation site was discovered at the base of papillary muscle in the five additional (100%) patients. **Conclusion:** NCM-guided localization of EA$_{SR}$ with Purkinje potential$_{(SR)}$ matches well with EA$_{VT}$ with Purkinje potential$_{(VT)}$ and provides an effective target for RFCA, potentially at the base of papillary muscle in patients with ILVT.

Key Words: Idiopathic left ventricular tachycardia, catheter ablation, non-contact map, Purkinje

INTRODUCTION

Belhassen, et al.[1] reported that idiopathic left ventricular tachycardia (ILVT) with right bundle branch block and left axis deviation responded to the intravenous in-

jection of verapamil. Macro-reentry within the Purkinje network along the posterior fascicle of the left ventricle (LV) is known to be a primary mechanism for ILVT,[2] and successful ablation of ILVT can be achieved at sites away from the tachycardia exit in some patients.[3] The earliest Purkinje potential has been suggested as an appropriate target for ablation.[4] Further, late diastolic potentials[4] preceding the Purkinje potential or Purkinje potential with presystolic potentials[5] have been demonstrated to provide the mechanism for ILVT and appropriate site for catheter ablation in patients with ILVT. However, it remains to be determined whether fascicular activation and Purkinje potential during sinus rhythm (SR; Purkinje potential$_{SR}$) can be a universal target for catheter ablation in patients with ILVT. If this site, mappable during sinus rhythm, plays a part in the reentrant circuit in patients with ILVT, it may provide an appropriate ablation target during sinus rhythm, especially in patients whose ILVT disappears during mapping by mechanical bump.[2] Recently, there have been several reports concerning the papillary muscle origin of VT;[6] however, its electroanatomical relationship with ILVT remains to be studied. Non-contact 3-dimensional mapping can record virtual unipolar electrograms, reflecting the direction of electrical impulse[7,8] with 3-dimensional anatomical correlations.[9-11] Therefore, we mapped the LV conductions of both sinus rhythm and ILVT with non-contact maps and analyzed their activation patterns and polarities on virtual unipolar electrograms with their anatomical relationships. We hypothesized that Purkinje potential$_{SR}$ and their preferential conduction to the LV, identified during sinus rhythm, are in close proximity to those observed during VT in patients with ILVT and, along with reentry anchors to the posterior papillary muscle, provide an appropriate target for radiofrequency catheter ablation (RFCA) during sinus rhythm.

MATERIALS AND METHODS

Patient characteristics and electrophysiologic study procedures

Among 19 patients with ILVT exhibiting a typical right bundle branch block morphology with a left axis (n=16) or right axis (n=3) deviation on surface ECG, 14 patients (age 35±13 years, 11 men; 3 women), in whom both VT and sinus rhythm had been successfully mapped using non-contact mapping (EnSite 3000 Ver. 4.2. St. Jude Medical Inc., Minnetonka, MN, USA), were included in the study. Also, five

additional patients were included for anatomical localization of successful ablation sites with echocardiogram, and two of them were confirmed simultaneously by computed tomography imported NavX imaging (St. Jude Medical Inc., Minnetonka, MN, USA). The study protocol was approved by the Institutional Review Boards and proper informed consent was obtained. Verapamil, beta-blockers and all antiarrhythmic drugs were discontinued for a period corresponding to at least five drug half-lives. No patient was taking amiodarone.

Intracardiac electrograms were recorded using the Prucka CardioLab™ Electrophysiology System (General Electric Medical System Inc., Milwaukee, WI, USA). A non-contact mapping balloon with a multi-electrode array was advanced through the left femoral artery and positioned in the LV using a retrograde trans-aortic approach, with stability ensured by using a 0.035" guide-wire positioned in the LV apex. After inserting the multi-electrode array into the LV, anticoagulation with heparin was started, maintaining an activated clotting time between 350 and 400 sec. The non-contact mapping technique and signal validations have been described elsewhere.[12] Three-dimensional geometry was obtained by maneuvering a steerable catheter (5 mm tip, Blazer II, Boston Scientific Inc., Natick, MA, USA) within the LV and sampling location points, under the guidance of fluoroscopy and electrograms. The LV posteroseptum was defined as the 6 to 9 o'clock region of the LV in the 35° left anterior oblique view and the middle third of the LV in the 35° right anterior oblique view.

Purkinje potential and their preferential conduction

We defined Purkinje potential as sharp fractionated potentials preceding the local ventricular electrogram at the LV posteroseptum (Fig. 1). The origin of the activation wavefront with high -dV/dt at the slow conduction zone was defined as the earliest activation site (EA), which manifested as a single white spot on the activation map of non-contact mapping. The breakout site on the same activation map of non-contact mapping was defined as the exit site that showed a sudden increase in the peak negative potential of the virtual unipolar electrogram after ventricular depolarization away from the EA.[13] Preferential conduction was defined as the initial direction of depolarization away from arrhythmic origin, when the EA was clearly separated from the exit site on the activation map[13] with reverse polarities of the virtual unipolar electrograms between the EA and exit site; i.e., QS to rS or rS to QS patterns (Fig. 2). Preferential conduction appears to be a part of the left posterior fascicle itself or ad-
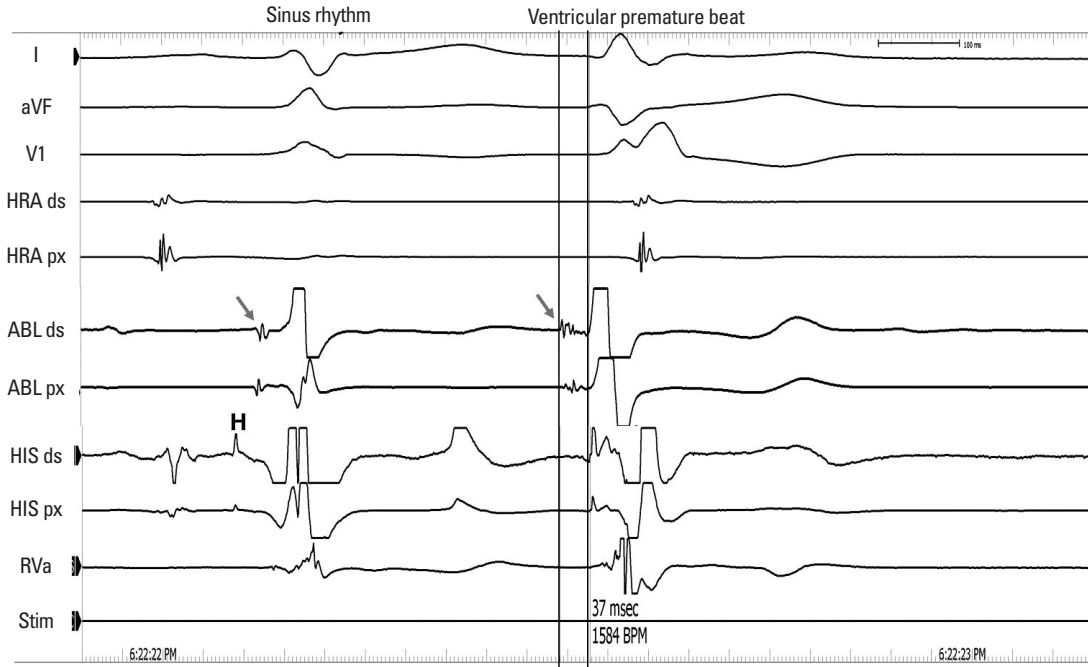
Fig. 1. Purkinje potential (arrows) during sinus rhythm and a ventricular premature beat with the same QRS morphology as ILVT. A sharp fractionated potential precedes the local ventricular potentials in the ablation catheter recordings (ABL). This Purkinje potential(SR) occurs later than the His potential (H), and the Purkinje potential(SR) to V interval (42 ms) is longer than Purkinje potential(VT) to the premature ventricular beat (37 ms). HRA and RVa stand for high right atrium and right ventricular apex. ds, distal; px, proximal. ILVT, idiopathic left ventricular tachycardia; ABL, ablation catheter; HRA, high right atrium; RVa, right ventricular apex.
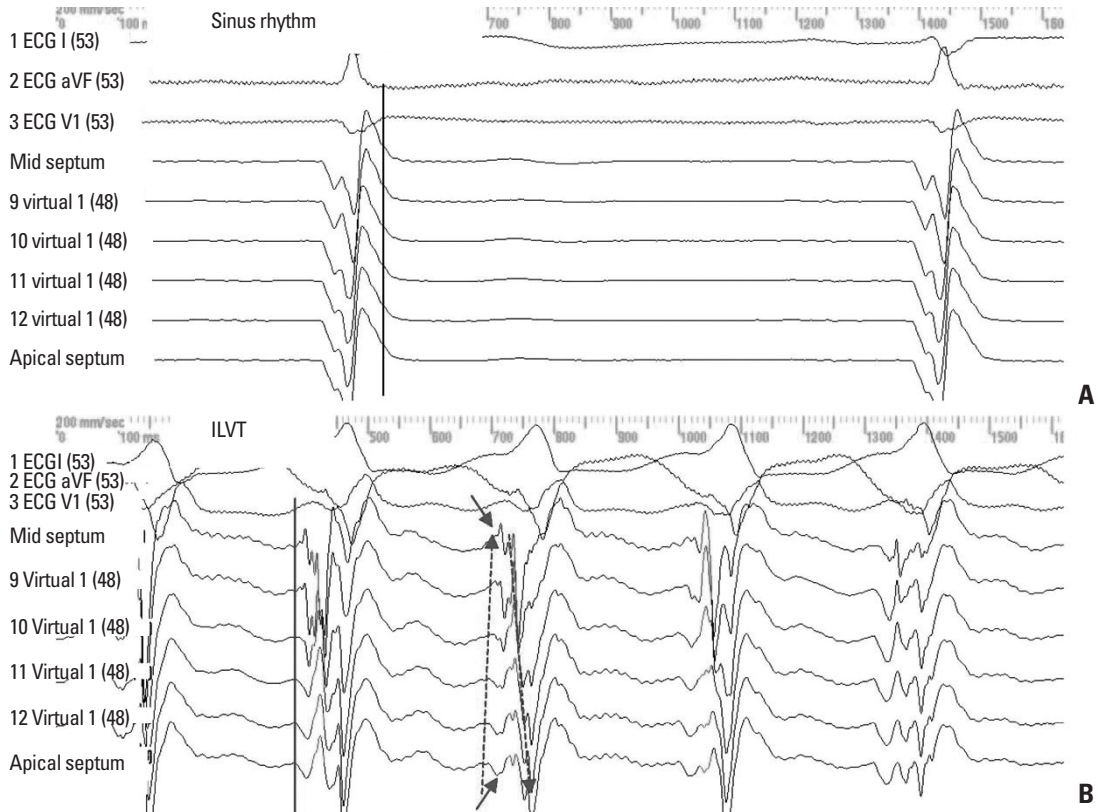

Fig. 2. Virtual unipolar electrograms during sinus rhythm (A) and ILVT (B) recorded at the LV posteroseptal region where Purkinje potential were recorded. The location of the virtual electrogram cursor matches that seen in the non-contact mapping in Fig. 4. The small notches preceding the ventricular potentials are on the mid-septum, and their polarities are respectively reversed during sinus rhythm and ILVT. In B, the QS pattern in the apical septum and the Rs pattern in the basal septum suggest that conduction through the posterior fascicle goes from the apical side to the basal side during ILVT. ILVT, idiopathic left ventricular tachycardia; LV, left ventricle.

jacent areas from the origin to exit site in macroreentry circuits.[5,14] We, at first, mapped LV activation patterns during sinus rhythm and ILVT. Then, we analyzed Purkinje potential (Purkinje potential$_{(SR)}$ and Purkinje potential$_{(VT)}$), preferential conduction patterns at LV posteroseptum (EA$_{SR}$-Exit$_{SR}$ and EA$_{VT}$-Exit$_{VT}$), and intervals between Purkinje potential and QRS onset during SR (Purkinje potential$_{(SR)}$-QRS) and VT (Purkinje potential$_{(VT)}$-QRS).

Catheter ablation

If a clear Purkinje potential$_{(SR)}$ was observed in the LV posteroseptum nearby and if EA$_{SR}$ was well-matched with EA$_{VT}$, EA$_{SR}$ was targeted for RFCA. EA$_{VT}$ was tagged on the geometry, and Purkinje potential$_{(SR)}$ was mapped in that area. If the conjunction points of the EA$_{VT}$ and Purkinje potential$_{(VT)}$ were separated from those during sinus rhythm, we targeted EA$_{SR}$. Radiofrequency (RF) energy (50W, 60°C for 60 sec, IBI 1500T, Irvine Biomedical Inc., Irvine, CA, USA) was delivered during sinus rhythm with a 5 mm tip deflectable ablation catheter (EP Technology Inc., Natick, MA, USA). In the five additional patients, the location of the ablation catheter at the successful ablation site was evaluated by 2D-echocardiography or computed tomography imported NavX imaging immediately before RFCA. The endpoint of ablation was noninducibility of VT with or without an isoproterenol infusion.

Data analysis

We analyzed surface ECGs and measured the cycle lengths of the VT, QRS width, intrisicoid deflection time, and QRS polarities in leads I, aVL and aVF, and compared them with the activation patterns and exit sites of VT on the non-contact mapping data. On the intra-cardiac electrograms, the interval between Purkinje potential and onset of QRS was measured and compared to those obtained during sinus rhythm (Purkinje potential$_{(SR)}$-QRS) and with those obtained during VT (Purkinje potential$_{(VT)}$-QRS). Bipolar contact electrograms from the ablation catheter were examined for activation timing relative to the onset of surface QRS (Fig. 1). We analyzed the activation patterns of VT and sinus rhythm and the corresponding virtual unipolar electrograms at the LV posteroseptum using non-contact mapping data. At the preferential conduction region, the polarity reversal patterns and location of the EA and exit sites were also compared during the ILVT and sinus rhythm. We measured the distance between the EA and exit sites via a frame-by-frame analysis of the non-contact mapping data and by using the virtual unipolar elec-

trograms. The conduction time was also measured using calipers on the virtual unipolar electrograms referenced to the activation map. The conduction velocities in the preferential conduction regions were calculated by dividing the distance between EA and exit by conduction time during the ILVT and sinus rhythm, respectively. All non-contact mapping analyses were performed with a 16 to 32 Hz high-pass filter setting in the discrete mode. Data were expressed as mean±SD. In order to compare the parameters during VT with those during sinus rhythm, a Student's t-test was used. A null hypothesis was rejected at $p < 0.05$.

RESULTS

Validation of the non-contact mapping virtual electrograms

The correlation between the contact and non-contact unipolar electrograms showed that the correlation coefficients of the voltage amplitude and time duration were 0.77 ($p < 0.001$) and 0.75 ($p < 0.001$), respectively (Fig. 3A and B). All 100 randomly selected points were within 35 mm from the center of the non-contact mapping balloon (24.9±5.1 mm). One percent of the validation points were found to be 2 SDs outside the mean amplitude of the contact unipolar electrogram within the LV using the Bland-Altman analysis (Fig. 3C). For the V wave duration difference, 3.0% of the validation points were outside of the 2 SDs (Fig. 3C and D).

Electrophysiologic characteristics of ILVT and polarity of Purkinje potential

Table 1 summarizes patient characteristics and clinical demographics. The ILVTs were primarily induced by ventricular extra-stimulation, but 3 ILVTs (21.4%) were induced by atrial pacing, and a VT was induced spontaneously. The mean VT cycle length was 357.1±40.2 ms and the mean QRS width was 113.4±19.3 ms. All induced ILVTs showed clear Purkinje potential$_{(VT)}$ in the contact bipolar electrograms (Fig. 1) and non-contact virtual unipolar electrograms (Fig. 2) at the LV posteroseptum. Purkinje potential$_{(SR)}$ were recorded at the LV basal to mid-posterior septum during sinus rhythm, except for one patient who did not show clear Purkinje potential$_{(SR)}$ during SR (Case #5 in Table 2). Table 2 summarizes the characteristics of the Purkinje potential and preferential conductions. During sinus rhythm, the intervals from the Purkinje potential$_{(SR)}$ to local V were longer (32.7±7.8 ms) than during VT (Purkinje potential$_{(VT)}$: 22.2±8.2 ms,

$p<0.02$) as measured in the bipolar electrogram. Purkinje potential$_{(SR)}$ demonstrated reversed polarity to Purkinje potential$_{(VT)}$ in the non-contact virtual unipolar electrograms (Fig. 2A and B). The directions of wavelets in the activation map at the region of the Purkinje potential$_{(SR)}$ and Purkinje potential$_{(VT)}$ were opposite to each other (Figs. 4 and 5). Pre-systolic potentials were observed when we increased the filter setting to 32 Hz and increased the voltage gain during VT (Fig. 4H) in 9/14 patients, while they disappeared with a lower filter setting (<16 Hz) or during SR.
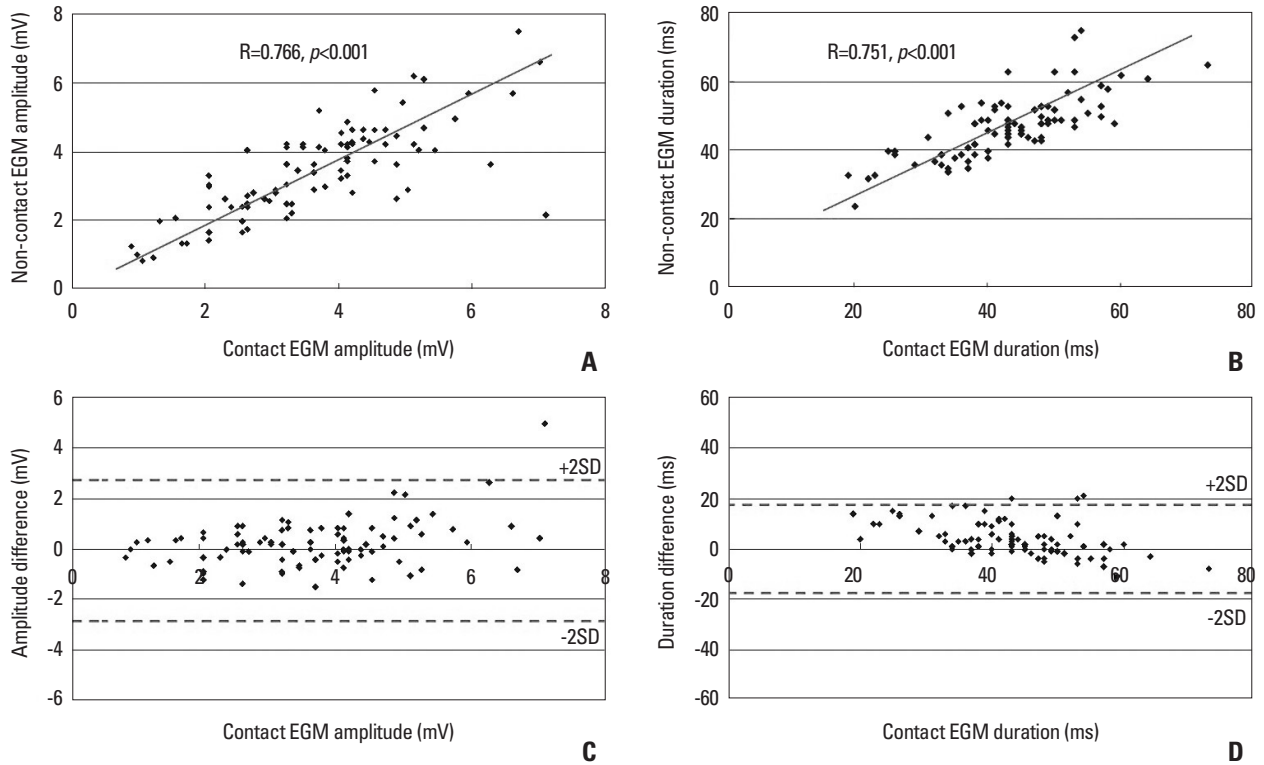

Fig. 3. Correlation curves (A and B) and a Bland-Altman analysis (C and D) showing the relationship between the contact and non-contact electrogram voltage amplitude (A and C) and time duration (B and D) in the LV. EGM, electrogram; LV, left ventricle; SD, standard deviation.

Table 1. Patient Characteristics and Clinical Variables

Patient No.	Sex	Age	VTCL (ms)	QRS width	Intrinsicoid deflection	Lead I	Lead aVL	Lead aVR	Induction mode	Procedure time (min)	Fluoroscopic time (min)	RF delivery number
1	M	38	364	131	67	Pos	Pos	Neg	RAP	220	95.6	3
2	M	19	436	89	38	Pos	Pos	Pos	VEST	100	29.6	5
3	M	16	353	117	42	Pos	Pos	Pos	VEST	150	48.5	3
4	M	29	364	101	80	Neg	Biph	Pos	VEST	150	44.6	3
5	M	28	383	97	31	Neg	Neg	Neg	VEST	240	83.5	6
6	F	32	363	108	53	Pos	Pos	Neg	RVP	180	55.0	5
7	M	33	358	141	95	Neg	Pos	Neg	RAP, VEST	155	31.0	4
8	M	40	394	103	48	Biph	Pos	Neg	VEST	160	75.2	3
9	F	65	364	120	88	Neg	Neg	Neg	Spont	355	119.5	7
10	M	37	310	99	42	Pos	Pos	Neg	VEST	180	30.3	3
11	M	54	318	85	39	Biph	Pos	Pos	VEST	185	NA	3
12	M	19	361	140	52	Biph	Pos	Pos	RAP	240	NA	4
13	M	33	264	142	49	Biph	Pos	Pos	RVP, VEST	180	NA	3
14	F	41	367	114	59	Pos	Pos	Neg	VEST	270	NA	6
		34.6 ±13.3	357.1 ±40.2	113.4 ±19.3	55.9 ±19.6					197.5±63.5	61.3±31.0	4.1±1.4

Pos, positive; Neg, negative; Biph, biphasic; RAP, rapid atrial pacing; VEST, ventricular extrastimulation test; Spont, spontaneous induction; RVP, rapid ventricular pacing; RF, radiofrequency; NA, not available; VTCL, ventricular tachycardia cycle length.

Table 2. Patterns of Polarity Reversal and Preferential Conduction

Patient No.	Purkinje-QRS (ms)		Polarity reversal	EA site		Exit site		EA to the exit during VT			EA to the exit during SR		
	VT	SR		VT	SR	VT	SR	(mm)	(ms)	(m/s)	(mm)	(ms)	(m/s)
1	24	35	PN	PS	Match	Apex	ApS	32	27	1.01	25	20	0.77
2	10	33	PN	Post	Match	ApS	Match	27	24	0.89	21	9	0.43
3	26	22	PN	PS	Match	ApL	ApS	26	59	2.27	29	33	1.14
4	26	36	PN	PS	Match	ApL	ApS	31	4	0.13	28	9	0.32
5	27	-	-	PS	Match	ApL	-	40	12	0.30	-	-	-
6	38	35	NP	PS	Match	ApS	ApP	15	12	0.80	19	32	1.68
7	13	27	NP	ApS	Match	ApL	PL	27	8	0.30	17	9	0.53
8	17	35	NP	PS	Match	ApS	Match	29	13	0.45	29	23	0.79
9	37	54	NP	PS	Match	ApS	PS	69	20	0.29	39	42	1.08
10	18	29	PN	PS	Match	Post	PS	23	36	1.57	18	15	0.83
11	15	31	PN	ApS	Match	Apex	ApL	22	15	0.68	19	6	0.32
12	22	33	NP	PS	Match	ApS	ApP	31	25	0.98	23	18	0.76
13	18	24	PN	ApS	Match	ApS	PS	23	75	0.68	10	4	0.40
14	20	31	PN	PS	Match	ApS	Apex	28	23	0.97	21	16	0.73
	22.2 ±8.2	32.7* ±7.8						30.2 ±12.6	25.2 ±19.9	0.80 ±0.57	22.9 ±7.2	18.2 ±11.6	0.75 ±0.38

VT, ventricular tachycardia; SR, sinus rhythm; PN, positive to negative polarity; NP, negative to positive polarity; EA, earliest activation site; PS, posteroseptum; ApS, apical septum; Post, posterior wall; ApL, apical lateral wall; PL, posterolateral wall; ApP, apical posterior wall.
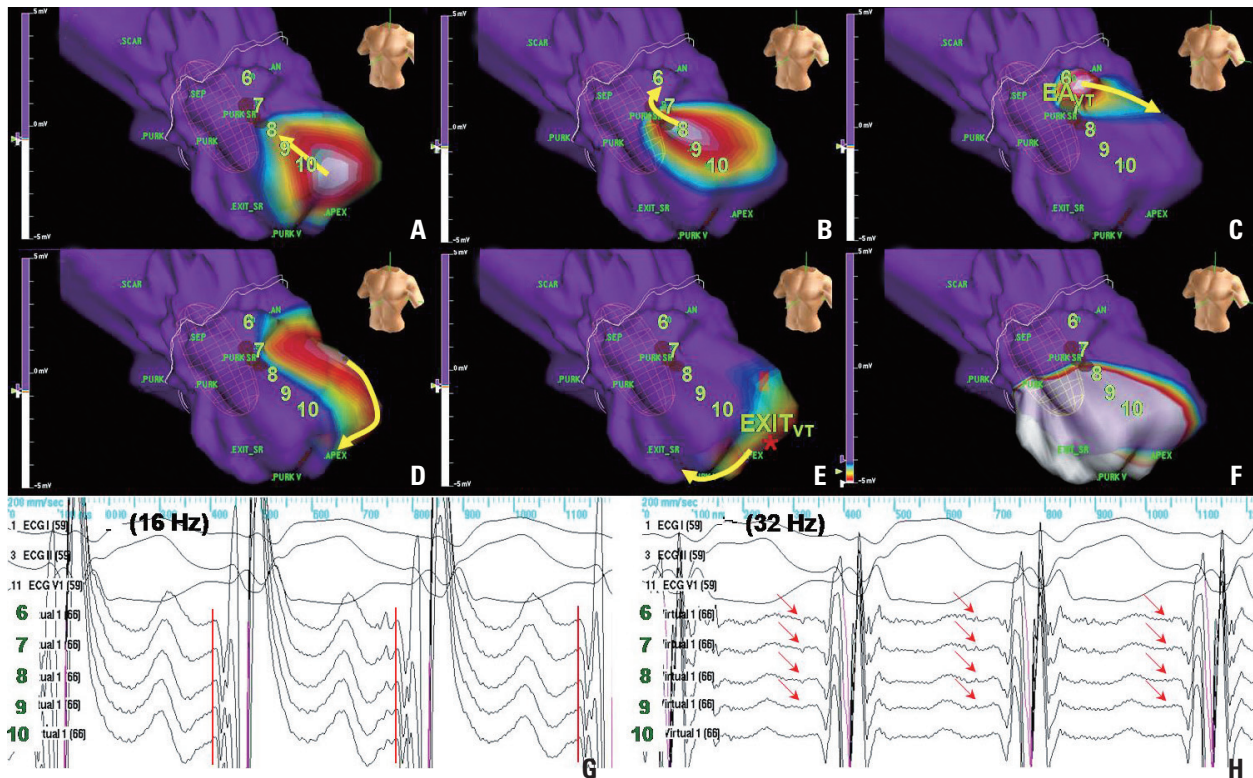*$p<0.02$.

Fig. 4. Activation pattern of an ILVT. The activation map (A-F) reveals retrograde conduction through the conduction system that reenters at a more mid-septal region. This reentry wavefront begins in this area (EA) and exits to the LV apex with preferential conduction. The sites of the numbers on the non-contact mapping mark the locations of the virtual electrodes recorded in panels G and H with the corresponding numbers. (G) Virtual electrograms with a 16 Hz filter setting recorded from the LV posteroseptum. (H) A high pass filter setting of 32 Hz shows pre-systolic potentials (arrows) at the conjunctional area of the Purkinje potential(VT) and EA(VT). This patient had QRS morphology of VT as a right bundle branch block and right axis deviation (case #5 in Table 1). ILVT, idiopathic left ventricular tachycardia; LV, left ventricle; EA, earliest activation site.

Preferential conduction pattern of ILVT and EA_SR

The activation map showed clear macro-reentry during VT (Fig. 4A-F) and a preferential conduction during both VT and sinus rhythm (Fig. 5A-F). The electrogram analysis also showed separated EA and exit sites that exhibited reversed polarity to each other in the unipolar electrograms during VT and sinus rhythm in all patients (Table 2). At the area showing a clear Purkinje potential$_{(SR)}$ at the LV posteroseptum, the location of the EA$_{SR}$ were in close proximity (5.8±8.2 mm) to EA$_{VT}$. However, the exit sites of VT were in the apical region, separated from EA$_{VT}$ by 30.2±12.6 mm during VT (Table 2). There was no significant difference in conduction time between that observed during VT and SR.

Catheter ablation and the imaging of papillary muscle

There was no mechanical touch-induced non-inducibility observed during the mapping. RF energy was delivered at EA$_{SR}$. We achieved acute success in all patients without any complication and the mean procedure time was 197.5±63.5 min. In the five additional patients, who were evaluated for the successful ablation site by imaging studies, the tip of the ablation catheter was on the base of posterior papillary muscle without exception (Fig. 6). All of these five patients had ECG findings of right bundle branch block and left axis deviation. None had recurrence of VT after 23.3±7.5 months of follow-up.

DISCUSSION

In this study, we proved that Purkinje potential during sinus rhythm and VT were easily determined by a non-contact mapping system. We found that the conjunction point of EA$_{SR}$ with Purkinje potential$_{(SR)}$ existed within close proximity to EA$_{VT}$ with Purkinje potential$_{(VT)}$, and provides an effective target for RFCA at the base of posterior papillary muscle in patients with ILVT. Non-contact mapping identifies activation through the Purkinje network or the fascicles responsible for reentry in the ILVT.

Purkinje potential and RFCA of ILVT

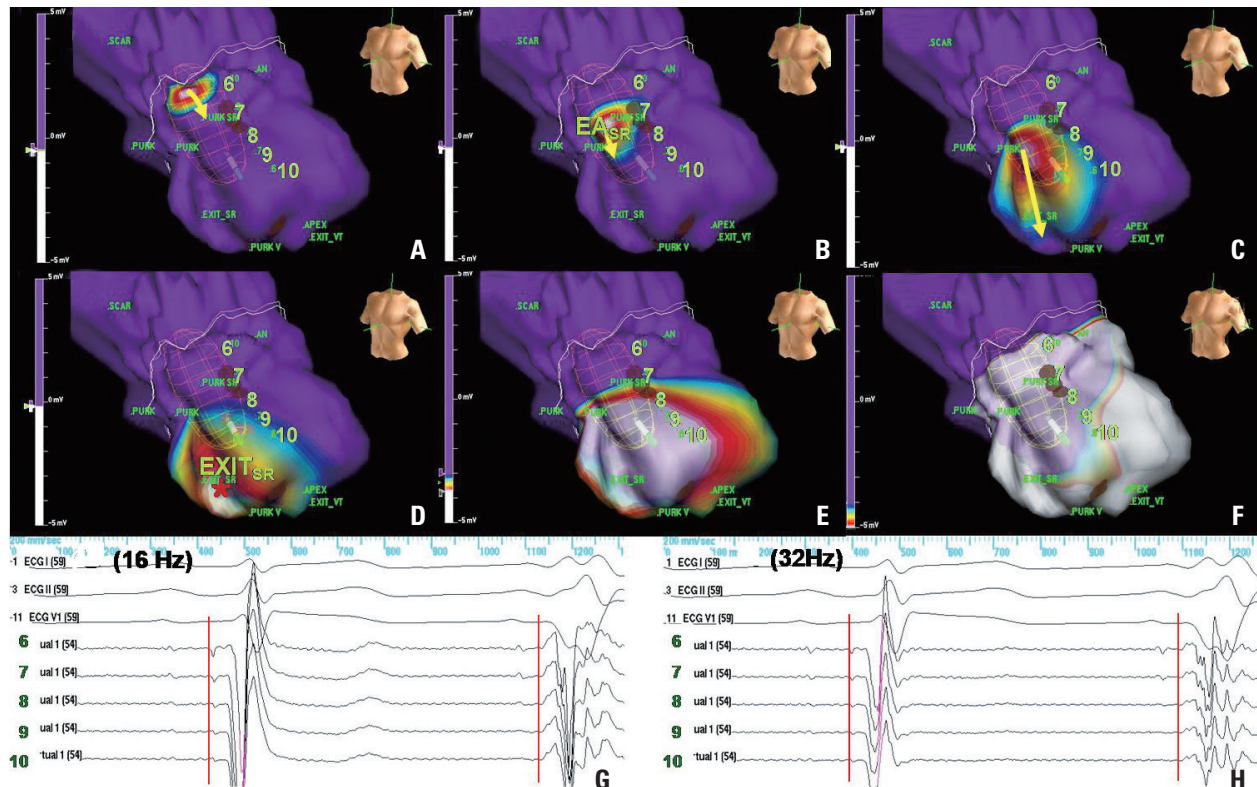It has been reported that a small macro-reentrant circuit con-

Fig. 5. Activation pattern during sinus rhythm in a patient with ILVT. The activation map (A-F) reveals anterograde conduction through the conduction system, which exits at the LV posteroseptum and apex. The EA$_{SR}$ is very close to EA$_{VT}$ (Fig. 4), and the exit sites were separated from each other (Fig. 4). G and H show the virtual unipolar electrograms of one beat in sinus rhythm and one in ventricular premature beat, recorded at the sites of the numbers on the non-contact mapping using 16 Hz and 32 Hz filter settings, respectively. The white, dotted circle stands for the potential location of papillary muscle estimated by comparing the left ventriculogram and non-contact map. ILVT, idiopathic left ventricular tachycardia; LV, left ventricle; EA, earliest activation site.
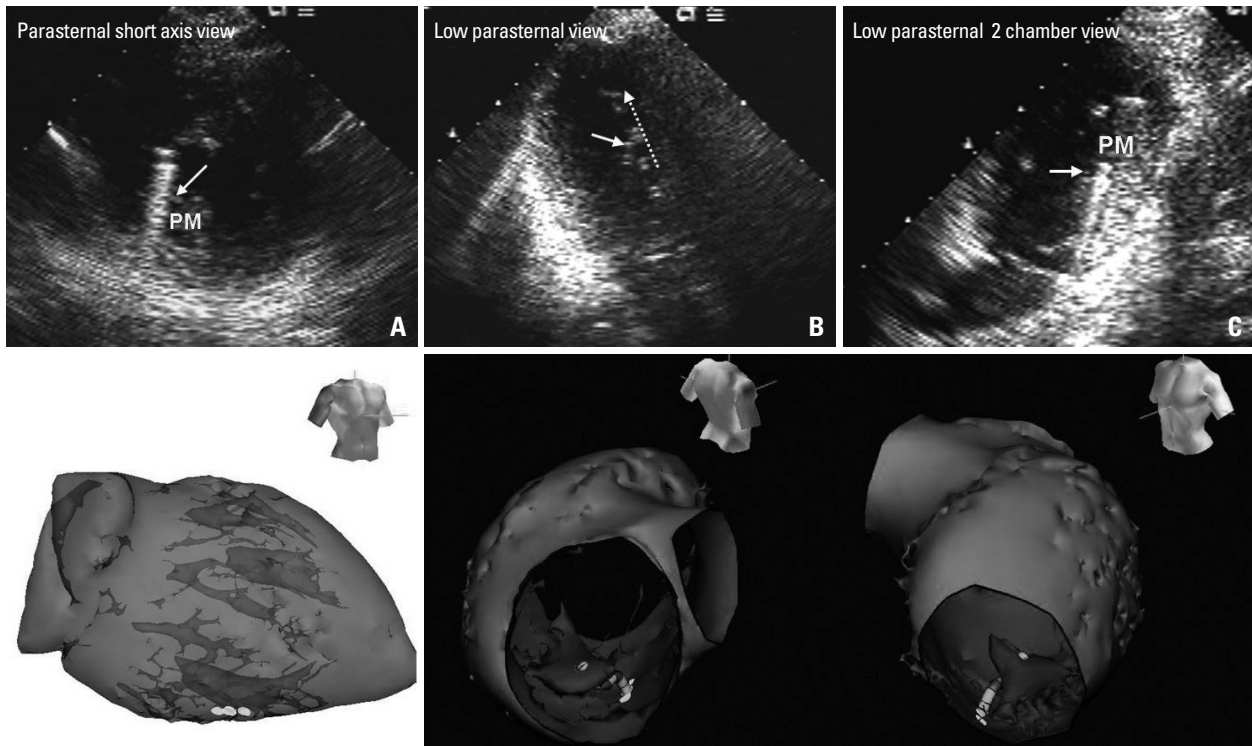
Fig. 6. Echocardiographic images (A, B, and C) show the relationship between posterior papillary muscle and the successful ablation site. These trans-thoracic echocardiographies were recorded during RFCA of ILVT, and the ablation catheter (white arrow) and decapolar catheter (white dotted arrow) were positioned in the LV. Lower panel: the ablation catheter is located close to posterior papillary muscle where the Purkinje and presystolic potentials were recorded. RFCA, radiofrequency catheter ablation; ILVT, idiopathic left ventricular tachycardia; LV, left ventricle; PM, papillary muscle.

fined to the posterior Purkinje system with an excitable gap and slow conduction is the main mechanism of ILVT.[2,5,15,16] Because this specific conduction system is surrounded by connective tissue that separates it from the ventricular myocardium, the Purkinje system can be identified by short, sharp, high-frequency potentials.[17] There have been several reports on the pre-systolic potentials at the site of the successful ablation in patients with ILVT, suggesting that these potentials represent the retrograde activation of a bystander Purkinje or fascicular fiber network.[2,5,16,18] However, it is sometimes difficult to record diastolic and presystolic potentials simultaneously at the ablation site during ILVT. Another difficulty of ILVT ablation is the disappearance of tachycardia during mapping by mechanical bump. Ouyang, et al.[2] reported that mechanical touch resulted in non-inducibility of ILVT lasting for longer than 2 hours, and that this was one of the major limitations of conventional mapping of ILVT and was associated with the recurrence of ILVT after ablation. He also reported that diastolic potentials during ILVT matched the earliest retrograde Purkinje potential during SR, and ILVT was successfully eliminated by targeting the retrograde Purkinje potential during SR without induction of VT in some patients.[2] There have been several reports of ILVT ablation utilizing Purkinje potential during SR.[19-21] In this study,

we systemically analyzed the locations of Purkinje potential and preferential conduction patterns (EA and exit) during SR and VT. We also proved their relationship with posterior papillary muscle. Non-contact mapping-guided localization of EA_{SR} with Purkinje potential$_{(SR)}$ matches well with EA_{VT} and Purkinje potential$_{(VT)}$ within 6 mm and provides an effective target for RFCA at the base of the posterior papillary muscle in patients with ILVT.

ILVT and posterior papillary muscle

Because Purkinje fibers are spread over the entire ventricular endocardium, it is unclear why reentry localized to the LV posteroseptum and the exit is located away from EA_{VT} in patients with ILVT. One potential explanation is that the macro-reentry of the ILVT is attributable to a reentry wavefront that is anchored to the posterior papillary muscle.[22] In the papillary muscle region without a direct Purkinje-muscular connection, Purkinje and papillary muscle potentials can be recorded separately,[23-26] and the activation from the Purkinje layer to the ventricular muscle layer occurs only at basal junctional sites.[26] Because the endocardial Purkinje potential are normally co-localized with the papillary muscle,[23] these findings suggest that reentry anchored near anatomical structures such as papillary muscles might also ac-

count for some cases of ILVT.[22] Purkinje potential$_{(VT)}$ are also present at the source of idiopathic ventricular fibrillation in humans.[27] We have previously reported that the papillary muscle serves as a significant anchoring point of reentry during propranolol-treated slow ventricular fibrillation in animal models and that RFCA at the papillary muscle significantly reduced the inducibility of the VF.[28,29]

Recently, there have been several reports of idiopathic VT successfully ablated from papillary muscle.[30,31] Although the nature of this specific type of VT is different from ILVT and based on automaticity, there is no clear-cut criterion differentiating ILVT and papillary muscle VT so far. We have demonstrated that successful ablation sites of ILVT were co-localized with posterior papillary muscle in 5 out of 5 patients in this study. We speculate that the weak electrical coupling between the Purkinje system and papillary muscle may induce automaticity in patients with papillary muscle origin VT, and anisotropy at the base of the papillary muscle and Purkinje network may contribute as a macroreentry circuit in patients with ILVT.

Clinical usefulness of NCM in ILVT ablation

Non-contact mapping has several merits for the mapping of ILVT. First, it can identify the global LV activation during sinus rhythm and VT without contacting the potential target site, even during a non-sustained episode or hemodynamically unstable state.[32] We did not experience mechanical touch-induced non-inducibility in any of the 14 patients in this study. Second, non-contact mapping detects the whole macroreentry circuit and reveals the direction of conduction with polarity patterns of virtual unipolar electrograms. At the high pass filter setting, non-contact mapping also detects Purkinje potential. Although Betts, et al.[11] reported that diastolic potentials were observed in only 20% of patients with ILVT utilizing non-contact mapping, they did not evaluate these at high pass filter settings. The 16-32 Hz high pass filter setting made non-contact mapping sensitive enough to identify small discrete potentials in this study. Third, the non-contact mapping balloon catheter positioned in the LV via the trans-aortic approach secured the ablation catheter from bouncing during each heartbeat.

Limitations

Although we validated the virtual unipolar electrograms using non-contact mapping, we recorded data obtained with the non-contact mapping instead of with contact electrograms. The virtual electrograms and activation maps of the non-contact mapping are complex and may be misleading, depending on the filter settings. Therefore, we kept the 16 to 32 Hz filter settings and analyzed the data from non-contact mapping with a single observer (the first author). In the analyses of electrogram polarity, 32 Hz high pass filtered virtual unipolar electrogram has a nature similar to bipolar electrogram so that it is hard to determine the direction of impulse propagation sometimes. Therefore, we always compared the electrograms at both 16 Hz and 32 Hz filter settings. We localized the successful ablation site by echocardiography in only 5 patients. Although all 5 patients with echocardiographically localized ablation site had a right bundle branch block with left axis deviation pattern of ECG morphology, 3 out of 19 patients had a right bundle branch block with right axis deviation pattern. We did not compare the difference of activation patterns during SR in normal control. We targeted EA$_{SR}$ instead of retrograde preferential conduction pathways during VT to find out the effective ablation site in SR map just in case of non-inducible VT.

Conclusion

We found that the conjunction point of EA$_{SR}$ with Purkinje potential$_{(SR)}$ existed within close proximity to EA$_{VT}$ with Purkinje potential$_{(VT)}$ and provided an effective target for RFCA on the base of the papillary muscle in patients with ILVT. Non-contact mapping identifies activation through the Purkinje network or the fascicles responsible for reentry in ILVT.

REFERENCES

1. Belhassen B, Rotmensch HH, Laniado S. Response of recurrent sustained ventricular tachycardia to verapamil. Br Heart J 1981; 46:679-82.
2. Ouyang F, Cappato R, Ernst S, Goya M, Volkmer M, Hebe J, et al. Electroanatomic substrate of idiopathic left ventricular tachycardia: unidirectional block and macroreentry within the purkinje

network. Circulation 2002;105:462-9.

3. Wen MS, Yeh SJ, Wang CC, Lin FC, Wu D. Successful radiofrequency ablation of idiopathic left ventricular tachycardia at a site away from the tachycardia exit. J Am Coll Cardiol 1997;30:1024-31.

4. Nakagawa H, Beckman KJ, McClelland JH, Wang X, Arruda M, Santoro I, et al. Radiofrequency catheter ablation of idiopathic left ventricular tachycardia guided by a Purkinje potential. Circulation 1993;88:2607-17.

5. Nogami A, Naito S, Tada H, Taniguchi K, Okamoto Y, Nishimura S, et al. Demonstration of diastolic and presystolic Purkinje potentials as critical potentials in a macroreentry circuit of verapamil-sensitive idiopathic left ventricular tachycardia. J Am Coll Cardiol 2000;36:811-23.

6. Doppalapudi H, Yamada T, McElderry HT, Plumb VJ, Epstein AE, Kay GN. Ventricular tachycardia originating from the posterior papillary muscle in the left ventricle: a distinct clinical syndrome. Circ Arrhythm Electrophysiol 2008;1:23-9.

7. Blanchard SM, Damiano RJ Jr, Smith WM, Ideker RE, Lowe JE. Interpolating unipolar epicardial potentials from electrodes separated by increasing distances. Pacing Clin Electrophysiol 1989;12: 1938-55.

8. Swartz JF, Tracy CM, Fletcher RD. Radiofrequency endocardial catheter ablation of accessory atrioventricular pathway atrial insertion sites. Circulation 1993;87:487-99.

9. Friedman PA, Asirvatham SJ, Grice S, Glikson M, Munger TM, Rea RF, et al. Noncontact mapping to guide ablation of right ventricular outflow tract tachycardia. J Am Coll Cardiol 2002;39: 1808-12.

10. Sra J, Bhatia A, Krum D, Akhtar M. Endocardial noncontact activation mapping of idiopathic left ventricular tachycardia. J Cardiovasc Electrophysiol 2000;11:1409-12.

11. Betts TR, Roberts PR, Allen SA, Morgan JM. Radiofrequency ablation of idiopathic left ventricular tachycardia at the site of earliest activation as determined by noncontact mapping. J Cardiovasc Electrophysiol 2000;11:1094-101.

12. Schilling RJ, Peters NS, Davies DW. Simultaneous endocardial mapping in the human left ventricle using a noncontact catheter: comparison of contact and reconstructed electrograms during sinus rhythm. Circulation 1998;98:887-98.

13. Higa S, Tai CT, Lin YJ, Liu TY, Lee PC, Huang JL, et al. Focal atrial tachycardia: new insight from noncontact mapping and catheter ablation. Circulation 2004;109:84-91.

14. Maruyama M, Tadera T, Miyamoto S, Ino T. Demonstration of the reentrant circuit of verapamil-sensitive idiopathic left ventricular tachycardia: direct evidence for macroreentry as the underlying mechanism. J Cardiovasc Electrophysiol 2001;12:968-72.

15. Okumura K, Matsuyama K, Miyagi H, Tsuchiya T, Yasue H. Entrainment of idiopathic ventricular tachycardia of left ventricular origin with evidence for reentry with an area of slow conduction and effect of verapamil. Am J Cardiol 1988;62:727-32.

16. Tsuchiya T, Okumura K, Honda T, Honda T, Iwasa A, Yasue H, et al. Significance of late diastolic potential preceding Purkinje potential in verapamil-sensitive idiopathic left ventricular tachycardia. Circulation 1999;99:2408-13.

17. Massing GK, James TN. Anatomical configuration of the His bundle and bundle branches in the human heart. Circulation

1976;53:609-21.

18. Tsuchiya T, Okumura K, Honda T, Iwasa A, Ashikaga K. Effects of verapamil and lidocaine on two components of the re-entry circuit of verapamil-senstive idiopathic left ventricular tachycardia. J Am Coll Cardiol 2001;37:1415-21.

19. Ma FS, Ma J, Tang K, Han H, Jia YH, Fang PH, et al. Left posterior fascicular block: a new endpoint of ablation for verapamil-sensitive idiopathic ventricular tachycardia. Chin Med J (Engl) 2006;119:367-72.

20. Lee KT, Chu CS, Dai ZK, Wu JR, Sheu SH, Lai WT. Successful catheter ablation of idiopathic left ventricular tachycardia during sinus rhythm. Int J Cardiol 2007;115:e74-7.

21. Chen M, Yang B, Zou J, Shan Q, Chen C, Xu D, et al. Non-contact mapping and linear ablation of the left posterior fascicle during sinus rhythm in the treatment of idiopathic left ventricular tachycardia. Europace 2005;7:138-44.

22. Chen PS, Karagueuzian HS, Kim YH. Papillary muscle hypothesis of idiopathic left ventricular tachycardia. J Am Coll Cardiol 2001;37:1475-6.

23. Joyner RW, Ramza BM, Tan RC. Effects of stimulation frequency on Purkinje-ventricular conduction. Ann N Y Acad Sci 1990;591: 38-50.

24. Kim YH, Xie F, Yashima M, Wu TJ, Valderrábano M, Lee MH, et al. Role of papillary muscle in the generation and maintenance of reentry during ventricular tachycardia and fibrillation in isolated swine right ventricle. Circulation 1999;100:1450-9.

25. Myerburg RJ, Nilsson K, Gelband H. Physiology of canine intraventricular conduction and endocardial excitation. Circ Res 1972; 30:217-43.

26. Veenstra RD, Joyner RW, Rawling DA. Purkinje and ventricular activation sequences of canine papillary muscle. Effects of quinidine and calcium on the Purkinje-ventricular conduction delay. Circ Res 1984;54:500-15.

27. Haïssaguerre M, Shoda M, Jaïs P, Nogami A, Shah DC, Kautzner J, et al. Mapping and ablation of idiopathic ventricular fibrillation. Circulation 2002;106:962-7.

28. Pak HN, Oh YS, Liu YB, Wu TJ, Karagueuzian HS, Lin SF, et al. Catheter ablation of ventricular fibrillation in rabbit ventricles treated with beta-blockers. Circulation 2003;108:3149-56.

29. Pak HN, Kim YH, Lim HE, Chou CC, Miyauchi Y, Fang YH, et al. Role of the posterior papillary muscle and purkinje potentials in the mechanism of ventricular fibrillation in open chest dogs and Swine: effects of catheter ablation. J Cardiovasc Electrophysiol 2006;17:777-83.

30. Good E, Desjardins B, Jongnarangsin K, Oral H, Chugh A, Ebinger M, et al. Ventricular arrhythmias originating from a papillary muscle in patients without prior infarction: a comparison with fascicular arrhythmias. Heart Rhythm 2008;5:1530-7.

31. Yamada T, Doppalapudi H, McElderry HT, Okada T, Murakami Y, Inden Y, et al. Electrocardiographic and electrophysiological characteristics in idiopathic ventricular arrhythmias originating from the papillary muscles in the left ventricle: relevance for catheter ablation. Circ Arrhythm Electrophysiol 2010;3:324-31.

32. Song PS, Kim JS, Shin DH, Park JW, Bae KI, Lee CH, et al. Electrical storms in patients with an implantable cardioverter defibrillator. Yonsei Med J 2011;52:26-32.